التحليل اللاخطي للأعتاب الخرسانية العميقة ذات مقاومة انضغاط خرسانية عالية باستخدام طريقة العناصر المحددة

الخلاصة:

في هذا البحث تم تحليل أربعة أعتاب خرسا نية عميقة ذات مقاومة انضغاط خرسا نية عالية تتراوح بين (86–120) ميكا باسكال مع استخدام قيم مختلفة لنسبة فضاء القص إلى عمق الأعتاب الخرسانية باستخدام طريقة العناصر المحددة للتحليل اللاخطي. تمت مقارنة النتائج للأمثلة المستخدمة والمستحصلة من التحليل اللاخطي للعناصر المحددة مع المدونة الأمريكية لسنة 2005 ومع النتائج المختبرية بشكل عام حصل توافق جيد بين النتائج المستحصلة من طريقة العناصر المحددة والنتائج المختبرية .اعتبر تصرف الخرسانة في الأنضغاط تصرفا (مرنا–لدنا) يتبعة تصرفا(تام اللدونة) ولغاية الفشل. أما سلوك الخرسانة تحت تأثير اجهادات الشد فقد تم تبني انموذج التشقق المنتشر مع الأخذ بالحسبان الاجهادات المتبقية في مرحلة ما بعد التشقق وتم استخدام أنموذج تصلب الشد(tension-stiffening model) كذلك استخدم أنموذج احتباس القص (shear retention model)لتخفيض قيمة معامل صلابة القص مع استمرار زيادة التشقق.وتم دراسة العديد من المتغيرات التي تخص العناصر المحددة ومعاملات تمثيل المادة.

1-Introduction

Deep beams are structural elements loaded as beams in which a significant amount of the load is transferred to the supports by a compression thrust joining the load and the reaction, also can be defined a beam having a ratio of span to depth of about (4) or less, or having a shear span (A) less than about twice the depth(ACI318, 2005). Reinforced concrete deep beams are commonly used in many structural applications including transfer girders, pile caps, foundation walls and offshore structures. Deep beams typically have low reinforcement ratios and may fail in tension, in compression or by splitting of the web as a result of excessive bursting forces. Reinforcement ratios in deep beams constructed with conventional strength concrete are generally low, and provided that the design is not limited by serviceability requirement. There is a scope for increased performance by increasing the area of steel reinforcement in conjunction with using higher strength concretes. With the growing use of high strength concrete, particularly in high rise structures and long span bridges. It is the aim of this paper to provide analytical data on single span high strength concrete deep beams and compared with experimental data (Stephen et.al.,1996).

The analytical data presented in this paper are compared with the design models of ACI 318M-05(ACI318, 2005).

The ACI design equations came from the empirical studies of Crist(Crist, 1967) and De Pavia and Siess(De Pavia et.al.,1965) (1965). The shear strength of deep beams in divided into a concrete component (**V_C**) and a steel component (**V_S**). The concrete component is given by:

$$V_C = v_c \, . b_w . d \tag{1}$$

Where v_c is the shear capacity given by:

$$v_C = \left[3.5 - 2.5\frac{Mu}{Vu\ d}\right]\left[0.16\sqrt{F'_C} + 17.2\ \rho w\frac{Vu\ d}{Mu}\right] \le 0.51\sqrt{F'_C} \tag{2}$$

where Mu and Vu are the ultimate moment and shear at the section under consideration, F'_C is the concrete strength in MPa, ρw is longitudinal reinforcement ratio($\frac{As}{b_w\ d}$),As is the area of longitudinal reinforcement and, **d** and **b_w** are the effective depth and beam width respectively.

The steel component is given by:

$$V_S = f_{sy}\ d\ \tan\emptyset\left[\frac{A_v}{s}\frac{1}{12}\left(1 + \frac{l_n}{d}\right) + \frac{A_{vh}}{s_h}\frac{1}{12}\left(11 - \frac{l_n}{d}\right)\right] \tag{3}$$

Where f_{sy} is the yield strength of the web reinforcement, A_v and $A_{vh}$are the vertical and horizontal web reinforcement respectively, **s** and s_h are the spacing of the vertical and horizontal web reinforcement respectively and tan $\emptyset$ is the apparent coefficient of friction.

and the capacity of the beam to carry shear is given by:

$$\mathbf{V_n = V_C + V_S} \le 0.68\sqrt{F'_C}\ \mathbf{b_w\ d} \tag{4}$$

$$\mathbf{Vu} \le \varphi\ \mathbf{V_n} \tag{5}$$

Where φ **i**s strength reduction factor equal to 0.75 for shear(ACI318, 2005).

2-Finite Element and Material Model:

The non-linear finite element approach can be used to predict the behavior of high strength reinforced concrete members at elastic stage, the cracking load, post-cracking stage and ultimate load. The approach can be considered as a theoretical or more accurately a numerical lab to test the high strength reinforced concrete members. The efficiency and accuracy of this lab depend mainly on suitable modeling of material properties of concrete and steel individually. Although this approach is widely used to analyze high strength reinforced concrete members .Three-dimensional non-linear finite element formulation is suitable for the analyses of high strength concrete member(Al-Shaarbaf, 1990).

The three dimensional modeling is adopted in the present study. The twenty-noded hexahedral isoparametric elements are used. The element has its own local coordinate system, r, s ,t shown in **Fig.(2)**, with the origin at the center of the element such that each local coordinate ranges from (-1) to (+1).

The concrete behaves as a linear elastic material when the stress level is less than about 30% percent of the uniaxial compressive strength, f_c' . This stress level is called the point of onset of localized cracking(Propvics, 1970).

For stress level ranging between 0.3 f_c' and 0.5 f_c' the stress-strain curve exhibits a slight non-linearity due to the extension of stress concentrations at the crack tips. When the stress level increases from 0.5 f_c' to 0.75 f_c', mortar cracks and other cracks continue and grow slowly with a gradual increase in the curvature of the curve(Chen, 1982).

Beyond this level of stress, the rate of crack propagation increases rapidly and the stress-strain curve bend sharply until the peak stress level is reached. Beyond the peak stress level, concrete shows a softening response, which presented by the descending portion of the stress-strain curve (Gerstle,1980).

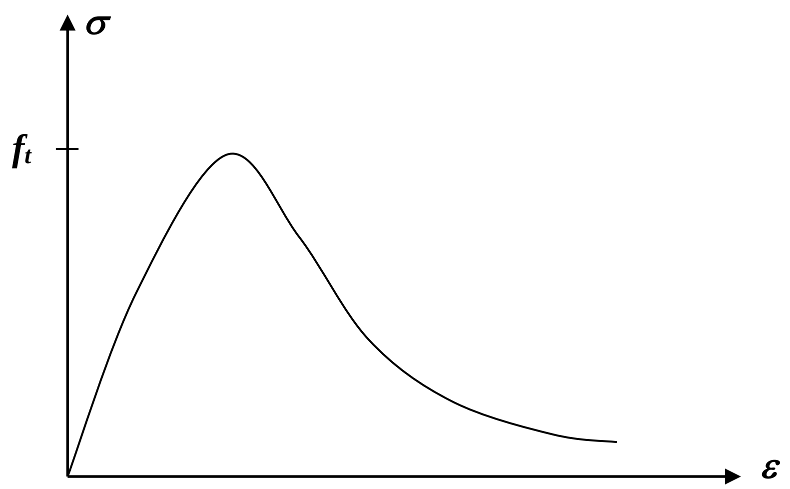

Fig.(1): Typical uniaxial stress-strain curve for concrete in tension.

Under uniaxial tensile stress, concrete exhibits a stress-strain curve similar, in shape, to that under compressive loading. The stress- strain response of concrete is linear up to a stress level of about 60 percent of cracking stress (f_t). Beyond this level, bond micro-cracks start to grow and non-linearity of the curve is started to increase as the stress level increases until peak stress is reached[(Chen, 1982)].

In the present study, a value of 0.3 is assumed for plastic coefficient C_p. The plastic yielding begins at a stress level of $C_p \ f'_c$. If $C_p = 1.0$, then the elastic perfectly plastic behavior is specified[(Al-Shaarbaf, 1990)].

Tension stiffening effect is found to be quite significant under service load conditions by increasing the overall stiffness of the system in the post cracking range.

In the finite element modeling of reinforced concrete two approaches have been suggested to account for this effects[(Pognani et.al.,1992)], the first approach is characterized by increasing the stiffness of steel bars. The second approach is characterized by a gradual decrease of the tensile stress in the cracked concrete over a specified strain range. Many researchers[(Al-Shaarbaf, 1990,Al-bahadly,1995, Allose,1995 and Al-Zahowi,1999)] used the second approach to account for the tension-stiffening effect in high strength reinforced concrete members, **Fig.(3)**.

The shear stiffness at a cracked sampling point becomes progressively smaller as the crack widens. So the shear modulus of elasticity is reduced to βG . Before cracking, the factor β is set equal 1.0. When the cracks propagate, the shear reduction factor (β) is assumed to decrease linearly, **Fig.(3)**[(Pognani et.al.,1992)].

In the present research work, the uniaxial stress-behavior of ordinary steel bars has been simulated by an elastic linear work hardening model, **Fig.(4)**.

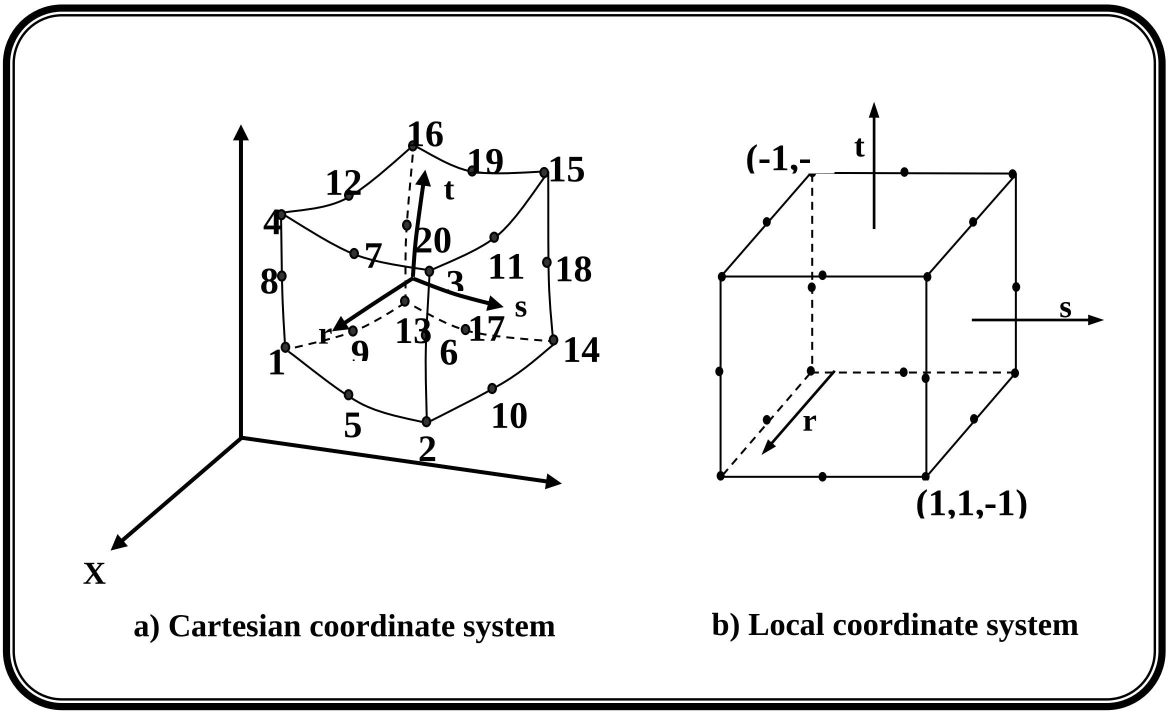

Fig.(2): the 20-noded isoparametric brick element coordinates

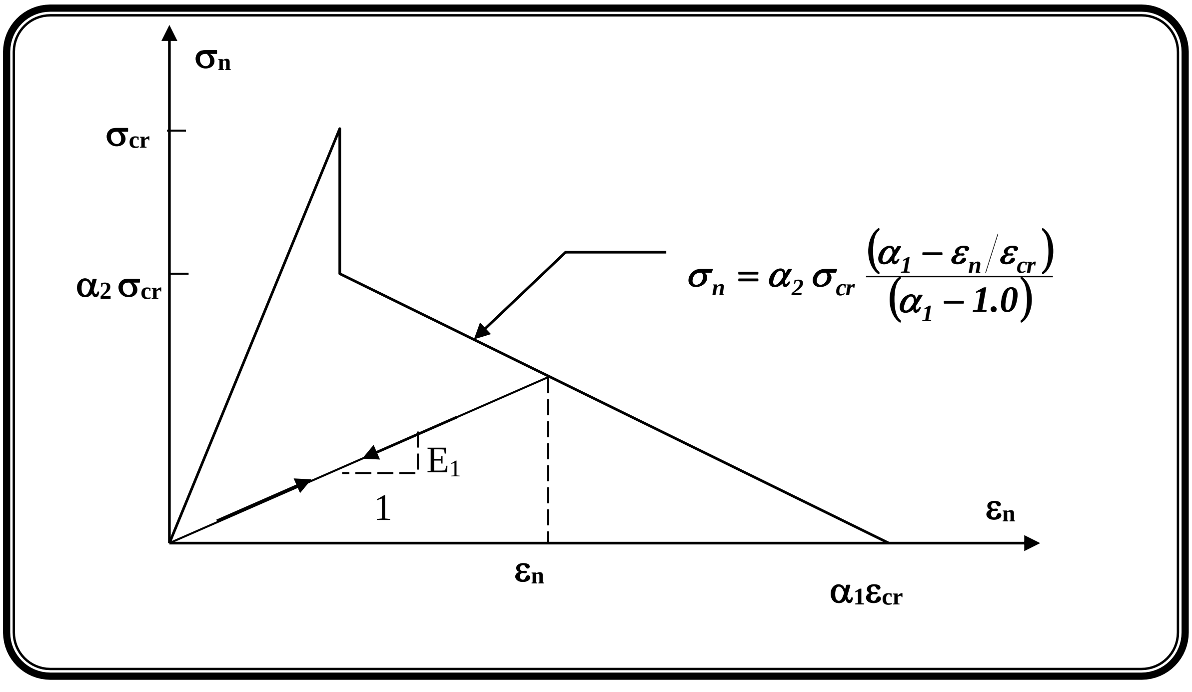

Fig.(3): tension stiffening model for concrete in tension(Al-Shaarbaf, 1990)

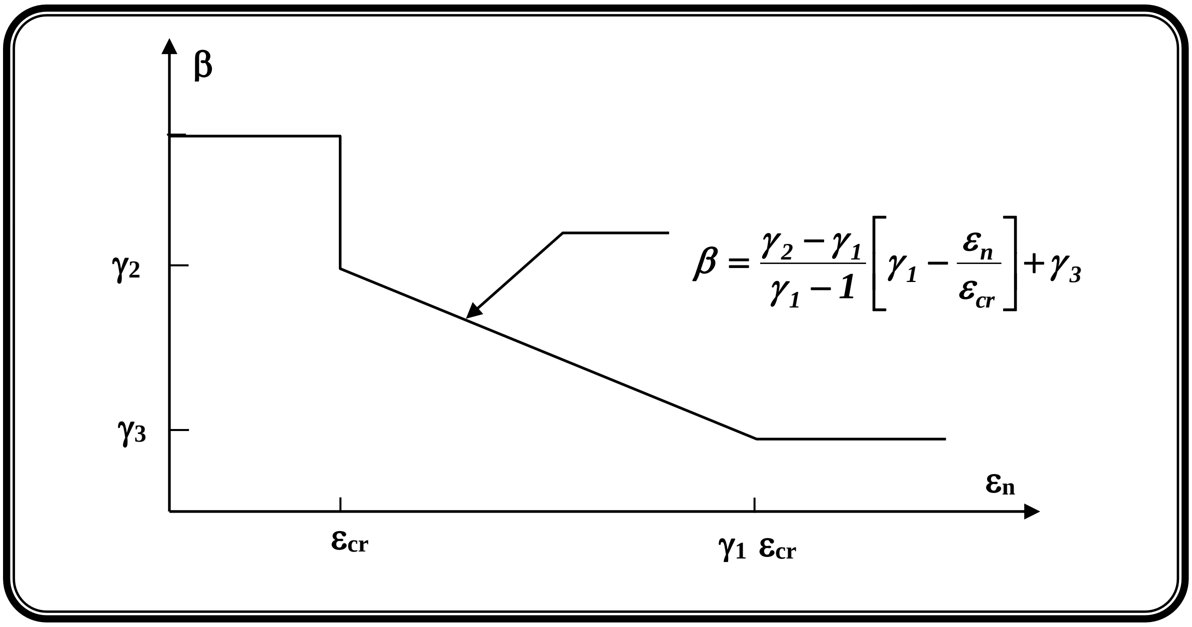

Fig.(4): shear retention model for concrete

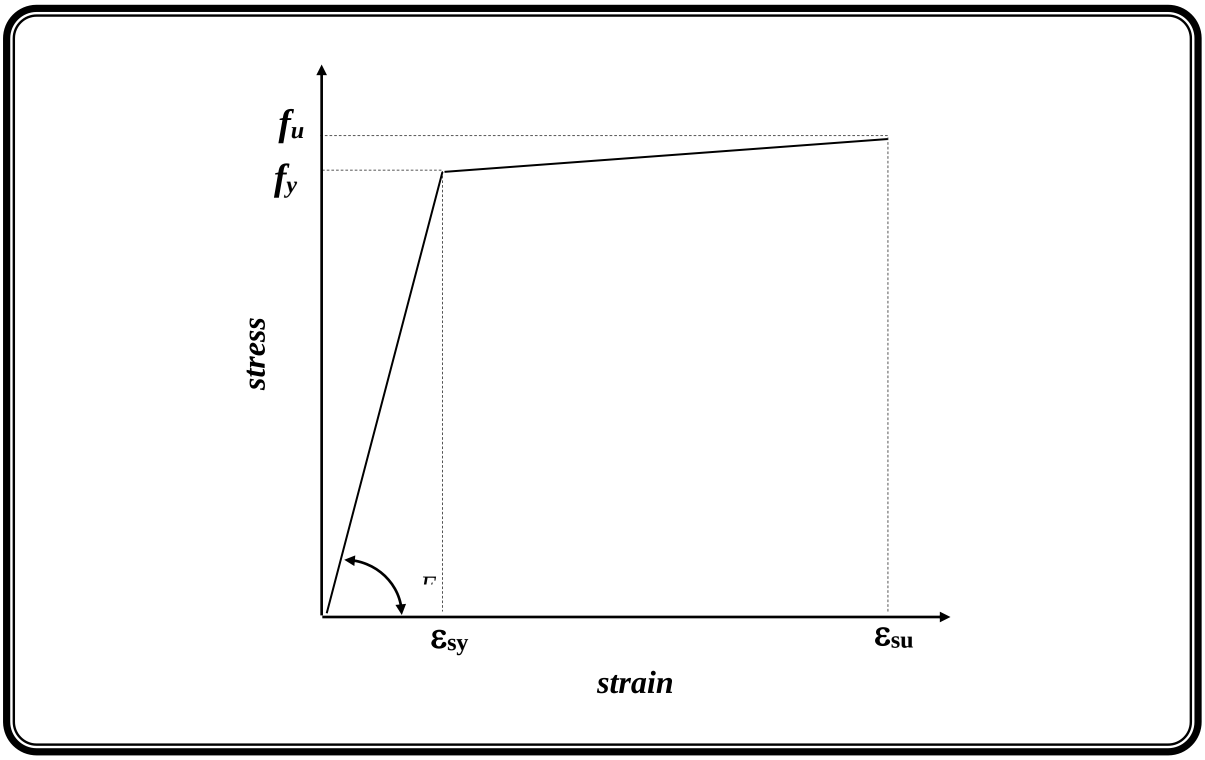

Fig.(5): stress-strain curve for ordinary steel bars used in the analysis

3- Nonlinear Finite Element Analysis of High Strength Concrete Deep Beams:

3-1 Introduction:

This section deals with the nonlinear finite element analysis of high strength concrete deep beams failing in a flexure-shear mode using a three-dimensional nonlinear finite element model. The ability of the constitutive models to simulate the behavior of high strength concrete deep beams is demonstrated through the analysis of four beams chosen from the available experimental studies. The specimens have been selected from 16 high strength concrete deep beams were tested to destruction from Stephen J. Foster B.E. et.al.(Stephen et.al.,1996). The results of the analyses of these examples are discussed and the load-deflection behavior obtained by the finite element analysis is compared with those obtained from the available experimental investigations.

3-2 Stephen J. Foster B.E. et.al. Deep Beams(Stephen et.al.,1996) :

In this paper 16 deep beams were tested with concrete strength ranging from (50 to 120 MPa) and shear span to depth ratios(a/d) from (0.5 to 1.32). Details of the test specimens are given in **Fig.(6)** and **Fig. (7)**.

The only four beams chosen to carry out the numerical tests were designated as B3.0-2, B2.0C-6, B2.0A-4 and B3.0A-4.

All concrete used in the study was supplied to the structures laboratory as ready mixed. The high strength concrete had a maximum aggregate size of 10 mm and consisted of a silica fume mix with superplasticizers added to improve workability.

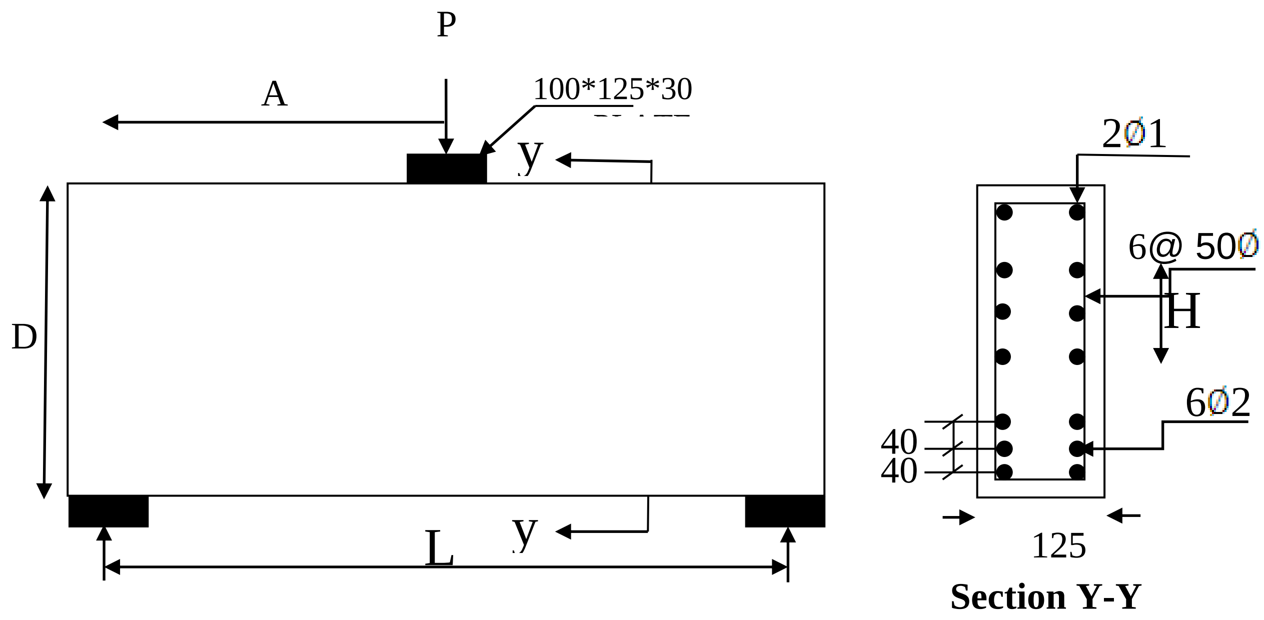

BEAM	Dimension in Millimeters			Web Reinforcement
	L	A	D	H
B2.0C-6	1400	825	700	-
B3.0-2	2100	1175	700	Ø6@135

Fig.(6): dimensions and details for beams B2.0A and B3.0A

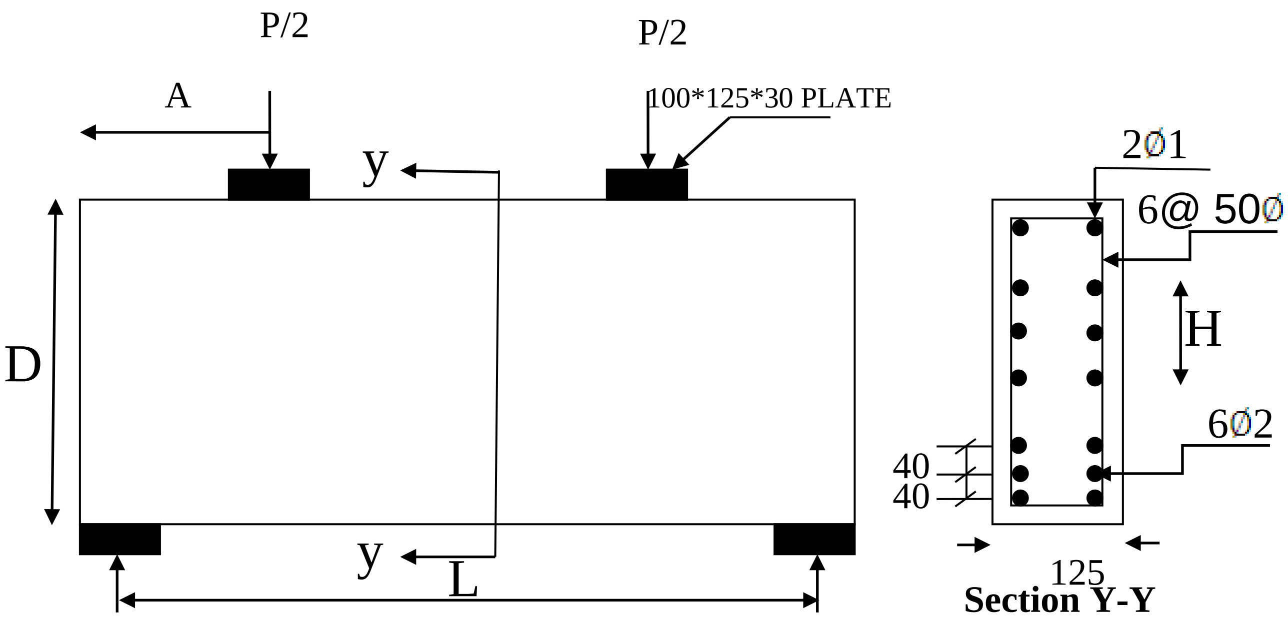

BEAM	Dimension in Millimeters			Web Reinforcement
	L	A	D	H
B2.0A-4	1400	675	700	Ø6@135
B3.0A-4	2100	925	700	Ø6@135

Fig.(7): dimensions and details for beams B2.0A and B3.0A

3-3- Finite Element Idealization of Deep beams B2.0C-6, B3.0-2, B2.0A-4 and B3.0A-4:

All length of beams has been used in the finite element analysis. The applied load was set as line load distributed across the width of the beam. The beam was modeled by using 20-noded brick element, The reinforcing bars are idealized as bar element embedded within the brick element as show in **Fig (8)**.

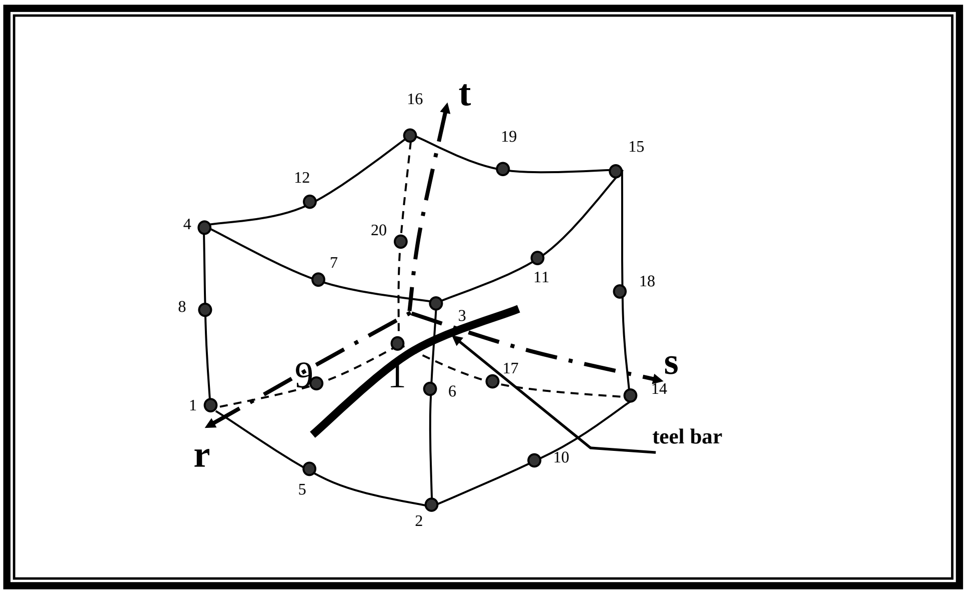

Fig.(8): the 20-noded brick element and embedded reinforcement in local coordinate system

The numerical tests have been generally carried out using the 27-point integration rule with a convergence tolerance of 3% then non-uniform increments have been used for applying the external loads. Large increments were used at the first stages of loading while appreciably smaller increments were used for stages close the ultimate load.

Table (1) shows the material properties and the adopted additional material parameters for deep beams B2.0C-6, B3.0-2, B2.0A-4 and B3.0A-4. **Fig.(9)** shows the finite element meshes for same deep beams.

Fig.(10) and **Fig.(11)** shows the Finite element idealization and boundary condition for deep beams B2.0C-6, B3.0-2, B2.0A-4 and B3.0A-4.

Table (1): Material properties and material parameters used for deep beams B2.0C-6, B3.0-2, B2.0A-4 and B3.0A-4

			B2.0C-6	B3.0-2	B2.0A-4	B3.0A-4
Concrete	Young's Modulus , (MPa)	E_c	50200	61400	50200	50700
	Compressive Strength, (MPa)	f_c'	93	120	86	88
	Tensile Strength , (MPa)	f_t	6.5	7.15	6.52	6.59
	Poisson's Ratio	ν	0.2	0.2	0.2	0.2
	Uniaxial Crushing Strain	ε_{cu}	0.005	0.007	0.0055	0.006
Web steel vertical and horizontal W6	Young's modulus (MPa)	E_s	193000	193000	193000	193000
	Yield Stress,(MPa)	F_y	590	590	590	590
	Diameter(mm)	D	6.3	6.3	6.3	6.3
Web steel horizontal Y12	Young's modulus (MPa)	E_s	195000	195000	195000	195000
	Yield Stress,(MPa)	F_y	440	440	440	440
	Diameter(mm)	D	11.9	11.9	11.9	11.9
Main longitudinal steel Y20	Young's modulus (MPa)	E_s	201000	201000	201000	201000
	Yield Stress,(MPa)	F_y	440	440	440	440
	Diameter(mm)	D	20	20	20	20
Tension-stiffening parameters	α_1		30	20	45	35
	α_2		0.55	0.5	0.65	0.55
Shear retention parameters	γ_1		15	10	15	15
	γ_2		0.5	0.5	0.55	0.5
	γ_3		0.13	0.1	0.15	0.13
Compressive strength reduction parameter	K_1		0.5	0.5	0.5	0.5
Biaxial material parameter	γ		1.16	1.16	1.16	1.16

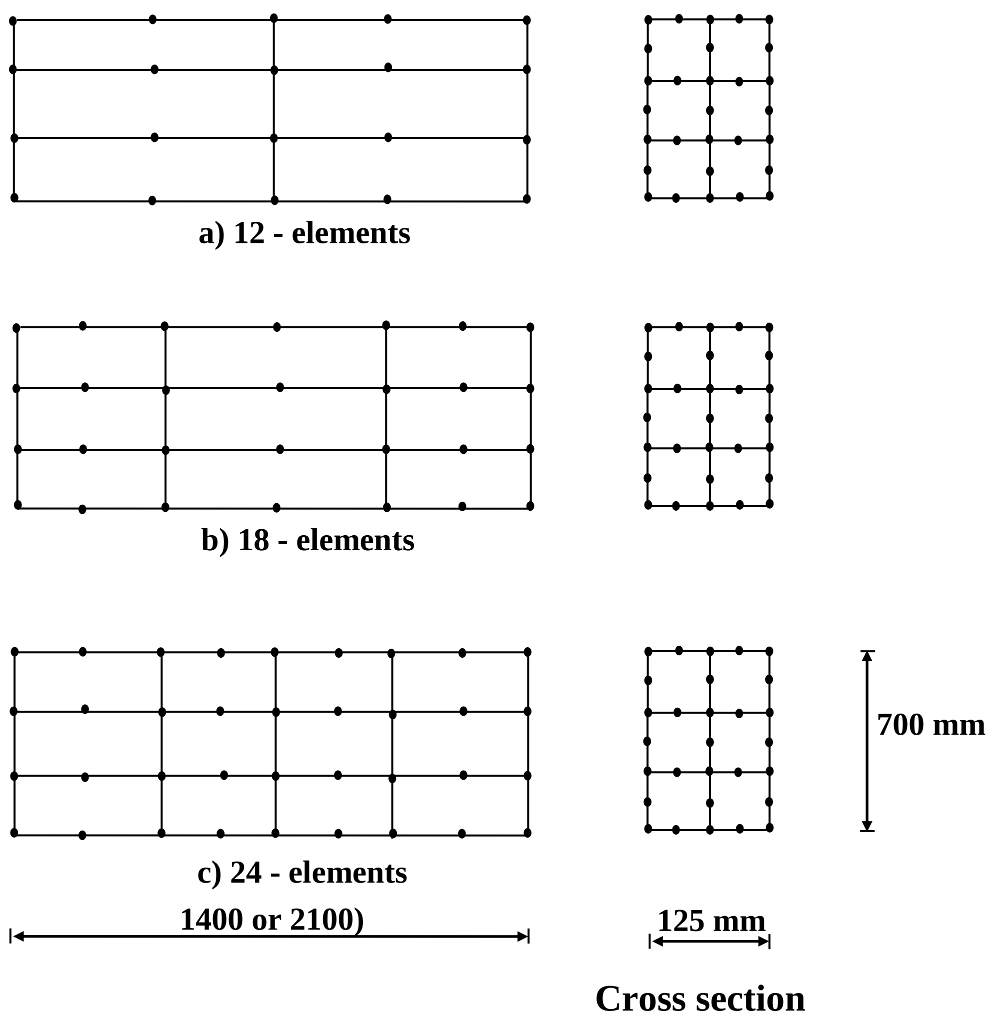

Fig. (9): finite element meshes for deep beams B2.0C-6, B3.0-2, B2.0A-4 and B3.0A-4

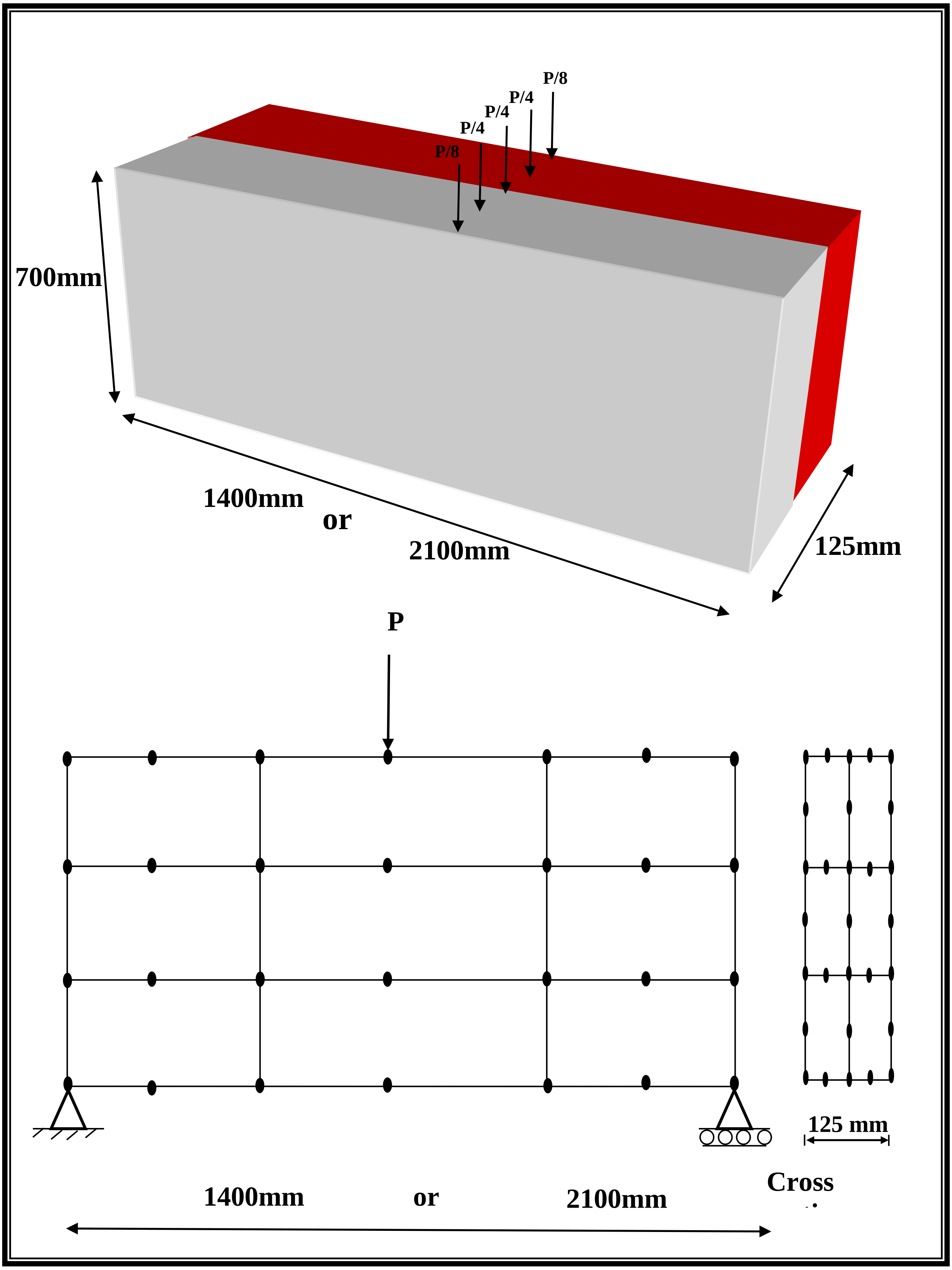

Fig.(10): finite element idealization and boundary condition for beams B2.0C-6 and B3.0-2

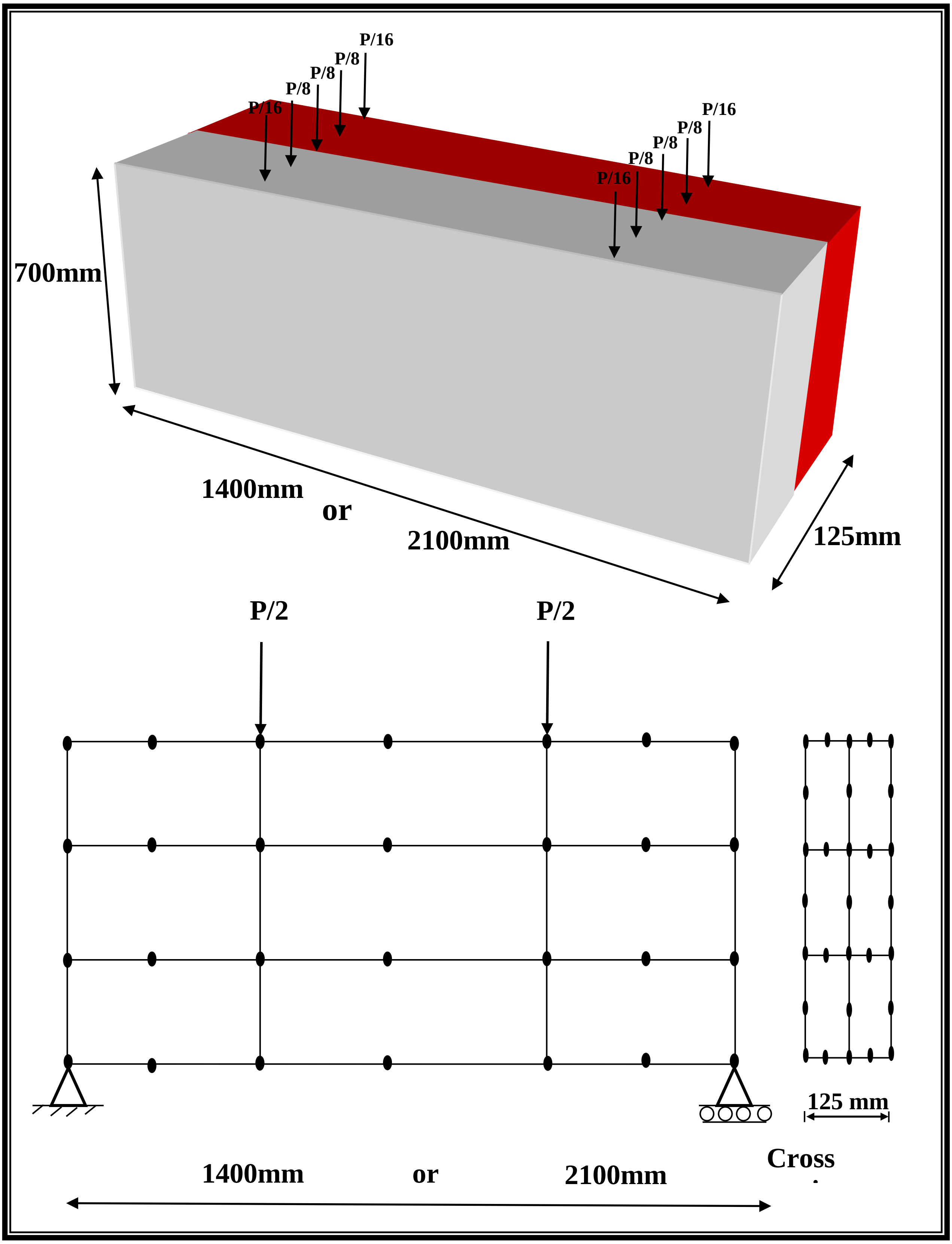

Fig.(11): finite element idealization and boundary condition for beams B2.0A-4 and B3.0A-4

3-4- Result of Analysis of Stephen J. Foster B.E. et.al. Deep Beams(Stephen et.al.,1996):

In this section, the results obtained by the finite analysis carried out for the chosen simply supported deep beams are presented and compared with experimental results(Stephen et.al.,1996). The experimental and analytical load-displacement curve for deep beams B2.0C-6, B3.0-2, B2.0A-4 and B3.0A-4 are shown in **Fig.(12)**, **Fig.(13)**, **Fig.(14)** and **Fig.(15)** respectively. Good agreement is obtained between the predicted numerical and the experimental load-displacement curve throughout entire range of behavior of the tested specimens.

Figures for deep beams B2.0C-6, B3.0-2, B2.0A-4 and B3.0A-4 show that both the initial and post-cracking stiffness are reasonably predicted. The computed failure loads were slightly higher than experimental failure load and the experimental and numerical mode of failure was a flexure-shear mode.

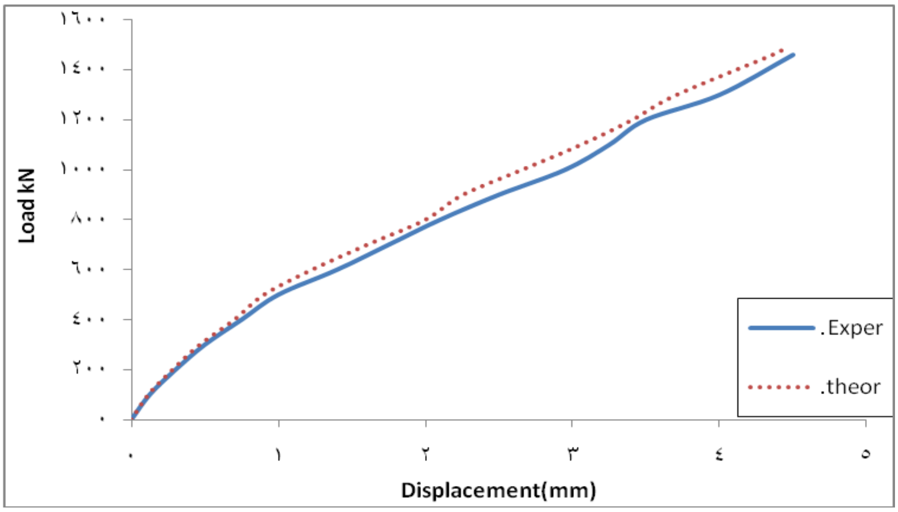

Fig.(12): numerical and experimental load-displacement curve of deep beam (B2.0C-6)

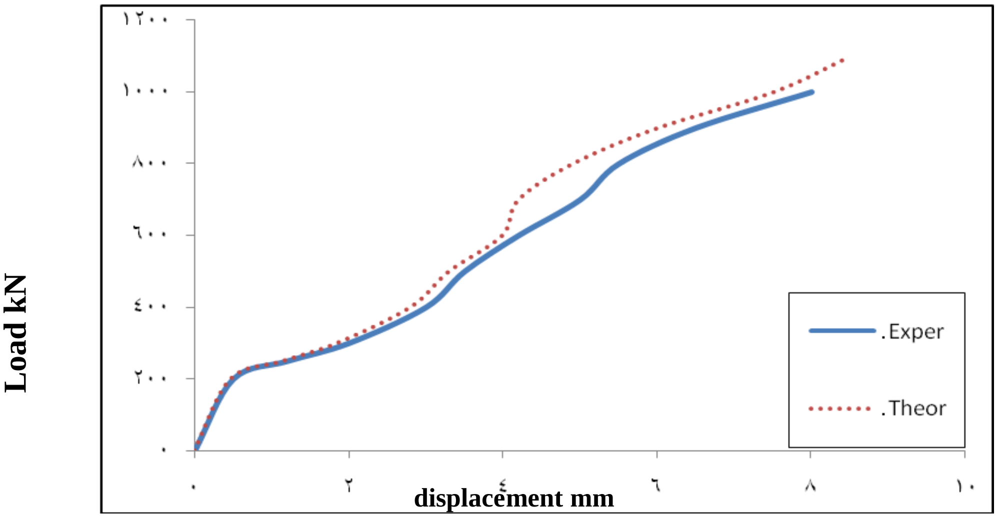

Fig.(13): numerical and experimental load-displacement curve of deep beam (B3.0-2)

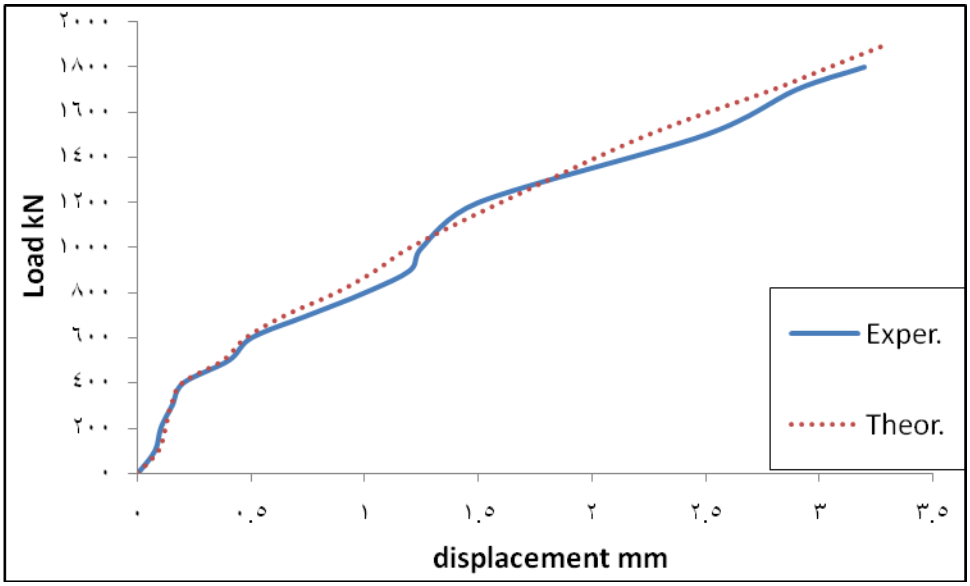

Fig.(14): numerical and experimental load-displacement curve of deep beam (B2.0A- 4)

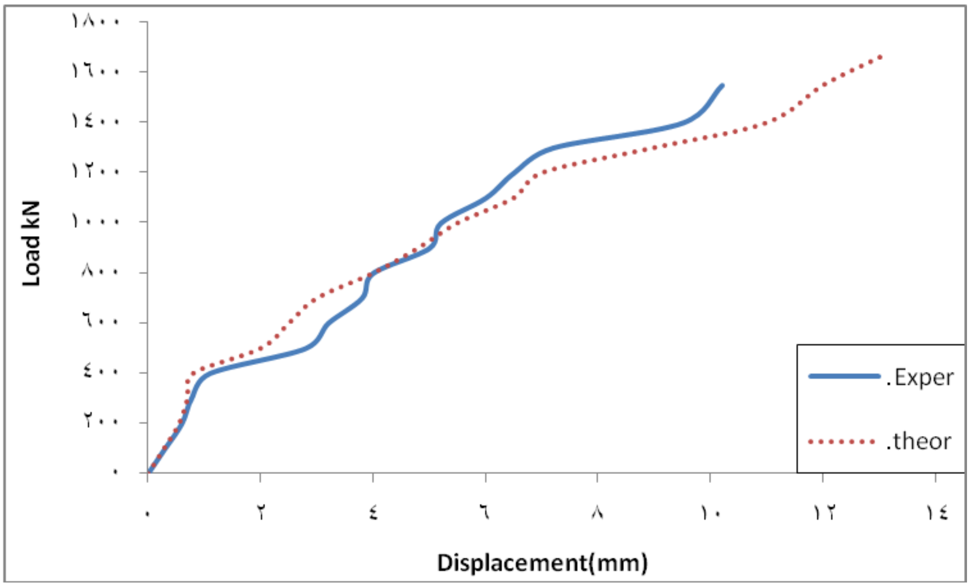

Fig.(15): numerical and experimental load-displacement curve of deep beam (B3.0A- 4)

4-Parametric Study for Deep Beam (B2.0A- 4) :

4-1- Effect of The Tension Stiffening Parameter (α_1):

The variation of the tension stiffening parameter α_1, which represents the rate of release of tension stress as the crack widens can strongly affect the post-cracking behavior of reinforced concrete beam under flexure. Numerical tests with values of α_1 equal to 25, 45, 65 have been carried out. In these tests the parameter α_2 was kept constant at 0.65. **Fig.(16)** indicates that the tension stiffening parameter α_1 affects the collapse load and the load-displacemen curve at early stages after cracking. A stiff response and higher load was occurred when α_1 was set equal to 65. The best fit to the experimental results was obtained when α_1 was set equal to 45.

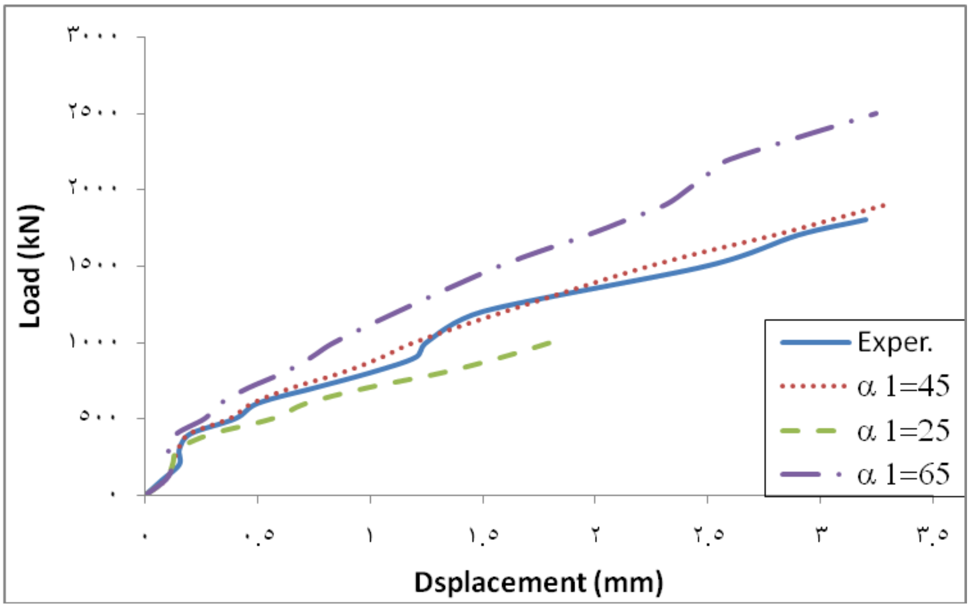

Fig. (16): deep beam (B2.0A- 4), parametric study of the tension stiffening parameter

4-2- Effect of The Tension Stiffening Parameter (α_2):

To study the effect of the tension-stiffening parameter α_2 which represents the sudden loss in the tensile stress at instant of cracking, numerical tests with values of α_2 equal 0, 0.5, 0.65 and 1.0 have been carried out. In these tests the parameter α_1 was kept constant at 45. The effect of the parameter α_2 on the load-displacement response is shown in **Fig.(17)**. The figure reveals that the parameter α_2 has a significant effect on the post cracking behavior and the ultimate load capacity. The best fit to the experimental results was obtained for α_2 equals to 0.65.

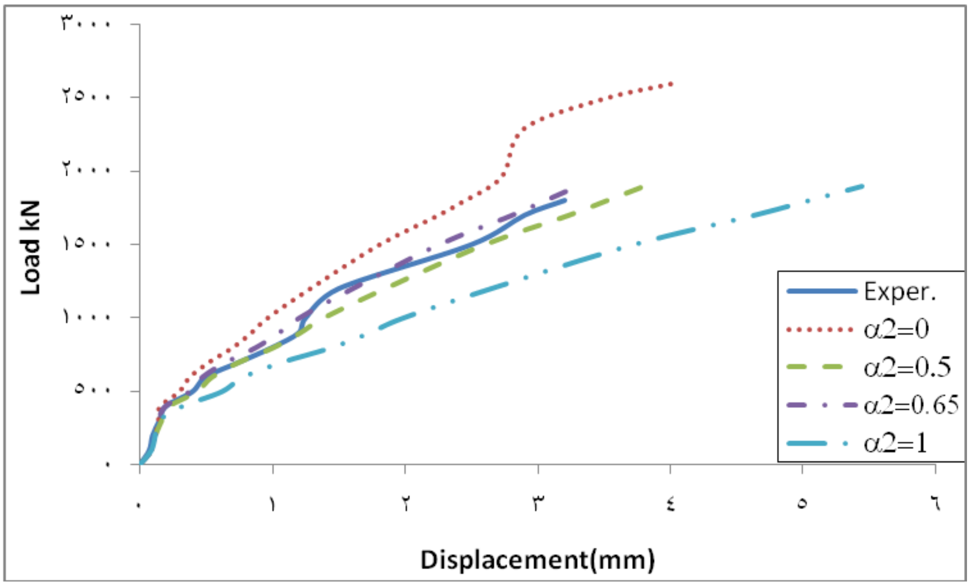

Fig. (17): deep beam (B2.0A- 4), parametric study of the tension stiffening parameter

4-3- Effect of Mesh Refinement :

For Stephen J. Foster B.E. et.al.(Stephen et.al.,1996) rectangular high strength reinforced concrete deep beam (B2.0A-4), three different finite element meshes have been considered to investigate the effect of the element aspect ratio as shown in **Fig.(18)** 12-elements, 18-elements and 24-elements . The numerical curves obtained using 12-elements has a slightly stiff response at the pre-cracking stage of behavior as compared with experimental work. However when the number of elements is increased, the numerical curves are in good agreement with the experimental results. in these test 18-elements has been used in all analyses carried out in this paper.

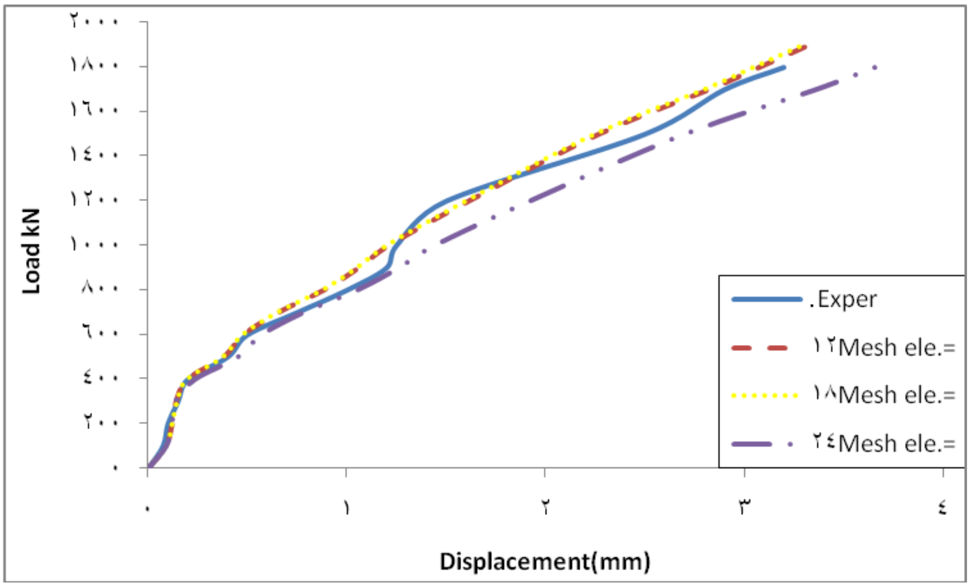

Fig. (18): deep beam (B2.0A- 4), parametric study of mesh refinement

4-4- Effect of High Compressive Strength of Concrete:

In order to study the effect of increasing the concrete compressive strength on the behavior and ultimate load capacity of high strength concrete deep beams, Stephen J. Foster B.E. et.al.[Stephen et.al.,1996] (B2.0A-4) has been analyzed for increased values of the concrete compressive strength. The concrete compressive strengths used in this analysis were, 107 MPa (1.25 f_c') , 129 MPa (1.5 f_c') and 215 MPa (2.5 f_c') where (f_c') is the experimental value (86 MPa) of concrete compressive strength. **Fig.(19)** shows the effect of increasing the compressive strength of concrete on the response of high strength concrete deep beams represented by the numerical load-displacement curves. It can be noted that a stiff response in the pre-cracking response and a slight increase in the ultimate load capacity is obtained when the value of compressive strength of concrete is increased. All predicted results for the load capacity are recorded in **Table (2)**.

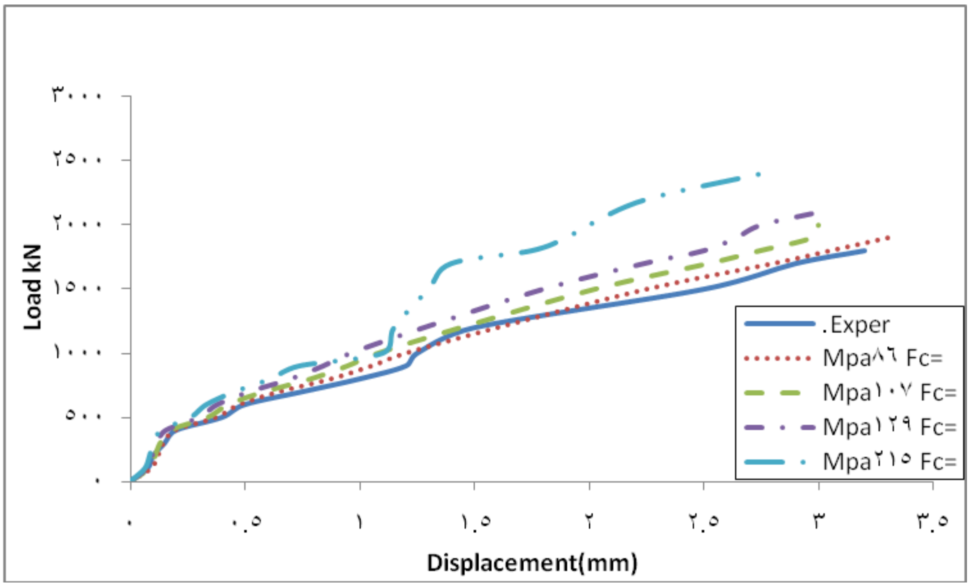

Fig. (19): deep beam (B2.0A- 4), parametric study of high compressive strength of concrete

Table (2): Stephen J. Foster B.E. et.al.(Stephen et.al.,1996) (B2.0A-4), ultimate load for different values of concrete compressive strength

	Experimental.(Stephen et.al.,1996)	Present Study			
Concrete compressive strength (MPa)	f'_c =86	f'_c =86	f'_c =107	f'_c =129	=215 f'_c
Ultimate load (kN)	1800	1900	2000	2100	2400
L. Numerical / L. Experimental	____	1.05	1.11	1.16	1.33

4-5- Effect of (Shear Span / Depth) Ratio:

To investigate the effect of using different (shear span/depth) ratios on the behavior of high strength reinforced concrete deep beams under to point load, Stephen J. Foster B.E. et.al.(Stephen et.al.,1996) beam (B2.0A-4) is analyzed with different (shear span / depth) ratios. For this study, a range of (shear span / depth) ratio between 0.8 and 1.3 for beam (B2.0A-4).

Fig.(20), compare the numerical results obtained for these ratios with the experimental curve, which represents the response of a (shear span / depth) ratio of about 0.96 for beam (B2.0A-4). Softer responses can be seen when the (shear span / depth) ratios are decreased .Also it can be seen that the predicted ultimate load capacity obtained is considerably decreased with the increase of this ratio. The ultimate loads obtained from this study for beam (B2.0A-4) are listed in **Table (3)**.

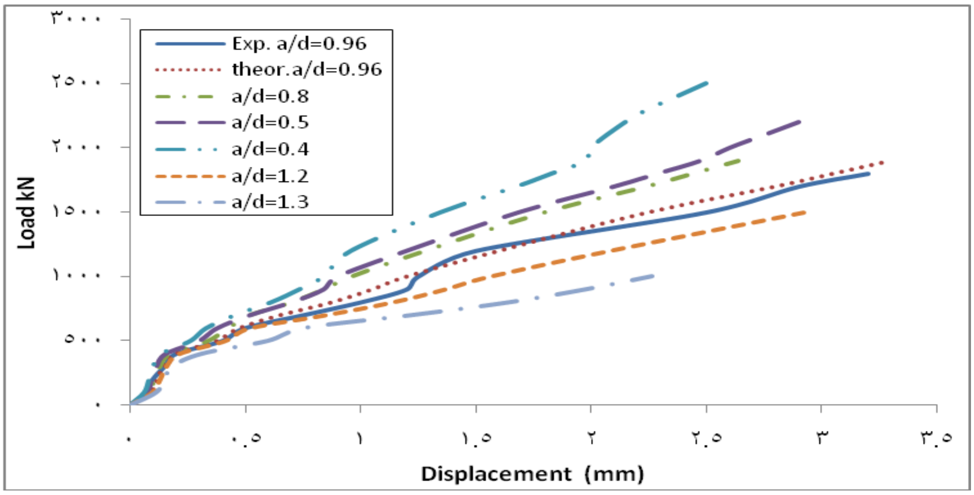

Fig. (20): deep beam (B2.0A- 4), parametric study of (shear span / depth) ratio

Table (3): predicted ultimate loads using different values of (shear span / depth) ratio for deep beam (B2.0A-4)

Shear Span / Depth Ratio, Beam (B2.0A-4)	ultimate load (kN)
Exp. a/d=0.96	1800
Theor. a/d=0.96	1900
Num. a/d=0.4	2500
Num. a/d=0.5	2200
Num. a/d=0.8	1950
Num. a/d=1.2	1500
Num. a/d=1.3	1000

4-6- Comparison of Results:

Table (4) compares the experimental results for deep beams with the theoretical results of ACI 318M-05(ACI318, 2005) and finite element method, in general the ACI 318M-05(ACI318, 2005) provision seem to be conservative.

Table (4): comparison of results

Specimen	Exp. Load $P_{u.exp.}$ (kN)	ACI 318M-05		Finite element method	
		$P_{u.a}$ (kN)	$\frac{P_{u.a}}{P_{u.exp.}}$	$P_{u.f}$ (kN)	$\frac{P_{u.f}}{P_{u.exp.}}$
B-2.0C-6	1460	934	0.64	1489	1.02
B3.0-2	1050	827	0.79	1100	1.05
B2.0A-4	1800	984	0.55	1900	1.055
B3.0A-4	1550	1087	0.70	1660	1.07

5-Conclusions:

1-Through comparing the experimental results for deep beams with the theoretical results of ACI 318M-05(ACI318, 2005) and finite element method, in general the ACI 318M-05(ACI318, 2005) provision seem to be conservative.

2- Softer responses can be seen when the (shear span / depth) ratio is decreased .Also it can be seen that the predicted ultimate load capacity obtained is considerably decreased with the increase of this ratio. The ultimate loads obtained from this study for beam (B2.0A-4) for **a/d=0.96, a/d=0.96, a/d=0.4, a/d=0.5, a/d=0.8, a/d=1.2 and a/d=1.3 are 1800 (kN), 1900 (kN),2500 (kN),2200 (kN),1950 (kN),1500 (kN)** and **1000 (kN)** respectively.

3-The effect of increasing the compressive strength of concrete on the response of high strength concrete deep beams represented by the numerical load-displacement curves. It can be noted that a stiff response in the pre-cracking response and a slight increase in the ultimate load capacity is obtained when the value of compressive strength of concrete is increased. The predicted results for the load capacity are **1800(kN),1900(kN),2000(kN),2100(kN)** and **2400(kN)** for compressive strength **86(MPa),86(MPa),107(MPa),129(MPa) and 215(MPa)** respectively.

4- The three-dimensional finite element model, which has been adopted in the present paper, is suitable to predict the behavior of High Strength Concrete Deep Beams. The numerical results are in good agreement with experimental load-displacement curves throughout the entire range of behavior.

6-Refrenses:

ACI Committee 318 Structural Building Code, “Building code Requirements for Structural Concrete and commentary (ACI 318-05)”, American Concrete Institute, 2005.

Al-bahadly, H. M. A., “Nonlinear Analysis of Elasto-Plastic Steel and Reinforced Concrete beams in Torsion using Three-Dimensional Finite Element model”, M. Sc. Thesis, University of Technology, Baghdad, 1995.

Allose, L. E. H., “Three-Dimensional Nonlinear Finite Element Analysis of Steel Fiber Reinforced Concrete beams in Torsion”, M. Sc. Thesis, University of Technology, Baghdad, 1995.

Al-Shaarbaf, I. A. S., ”Three-Dimensional Non-Linear Finite Element Analysis of Reinforced Concrete Beams in Torsion”, Ph.D. Thesis University of Bradford, 1990.

Al-Zahowi, S. K., “Nonlinear Finite Element Analysis of Reinforced Concrete Voided Slab Strips”, M. Sc. Thesis, University of Technology, Baghdad, 1999.

Chen, W. F., “Plasticity in Reinforced Concrete “, Mcgraw-Hill, 1982.

Crist R.A., Shear behavior of deep reinforced concrete beams, Vol. 2 , static tests, AFWL-TR-67-61,Kirkland Air Force Base,N.M.,Oct.1967.

de Pavia, H.A.R. and Siess, C.P., Strength and behavior of deep beams in shear. ASCE Proceedings, Oct 1965.

Gerstle, K. H., “Behavior of Concrete under Multiaxail Stress State”, Journal of the Structural Engineering Division, ASCE. Vol. 106, No. 6, December 1980.

Pognani, T., Slater, J., Anneur-Mosor, R. and Boyukozurk, O., “A Nonlinear Three-Dimensional of Steel Fiber Reinforced Concrete based on Bounding Surface Model”, Journal of computer and Structures, Vol. 43, No. 1, 1992.

Propvics, s., “A Review of Stress-Strain Relationships Concrete”, ACI. J., Vol. 67, No. 3, March 1970.

Stephen J. Foster B.E., MEngSC., PhD. And R.lan Gilbert B.E.,PhD., ”Tests on High Strength Concrete Deep Beams”, The University of New South Wales, Sydney, Australia, 1996.